

Off-Design Performance Prediction of the CFM56-3 Aircraft Engine

Daniel Alexandre Rodrigues Martins
daniel.r.martins@tecnico.ulisboa.pt

Instituto Superior Técnico, Lisboa, Portugal

November 2015

Abstract

Ever since the appearance of aircrafts in the beginning of the past century, they have been transforming the world. Their capability of travelling at speeds much greater than that of trains or ships helped the world by facilitating the economic trade and helped people to learn about other cultures. The overall performance of a gas turbine can be estimated by knowing the main design parameters, however, this is quite challenging due to the limited data that the engine manufacturer releases to the general public. Although a turbine manufacturer usually provides data about the turbine interface, the data required to estimate the thermodynamic cycle of a particular gas turbine remains hidden. A model of that engine capable of estimating that data must then be created. In this thesis, a performance model of the CFM56-3 engine has been developed using a modelling software called GasTurb. The chosen engine was the CFM56-3 due to the facts that it is one of the world's most used aircraft engines and that TAP M&E Engine Shop is certified to maintain it. The model is first created for its design point, where its geometry is defined. The Off-design performance of the engine is then modelled using data from TAP M&E test bed. The model is useful to predict the data that the engine manufacturers do not reveal. The best application of this work is the analysis of the condition of CFM56-3 engines. With some test bed data from a particular engine, the model might diagnose the problems of that same engine. The thesis places major emphasis on the development and validation of the engine model, as well as its use in TAP M&E Engine Shop. The developed model allows TAP M&E to analyse the performance of the gas turbine as well as to compare the performance of any CFM56-3 engine to the performance of the model in order to estimate components degradation. The main benefit to TAP M&E by using the performance model is the possibility of performing selective repairs, allowing to save work hours and reducing the repair costs.

Keywords: Gas turbine, Thermodynamics, Performance model, GasTurb, Degradation effects, Repair costs, Tip clearance.

1. Introduction

The phenomenon of deterioration in gas turbine engines can make their operation uneconomical to airline companies as well as unsafe and untrustworthy for their clients. That fact leads to a requirement, a proper knowledge of the true state of the gas turbine is essential.

The knowledge of the behaviour of a gas turbine leads to early detection of the cause of deteriorations or failures of its components, which allows appropriate maintenance activity to be undertaken to restore the engine performance and/or ensure safe operation. These operations are the responsibility of Maintenance, Repair and Overhaul (MRO) companies such as TAP Maintenance & Engineering.

TAP M&E is interested in understanding the degradations affecting the engines throughout their life time and what effects those degradations bring,

specifically two degradations in the High Pressure Compressor (HPC) blades: chord length reduction and tip clearance increase.

The goal of this thesis is firstly to model the CFM56-3 engine in the software GasTurb, a commercial engine performance modelling software. The model will be used for estimating the engine performance by comparing it to engine performance data from the engine tested in reference [1]. Secondly, apply the tuned model to test cases from engines that had shop visits in TAP M&E facilities, studying their degradation and the effects on the overall efficiency of the engine. Lastly, the model will be used to study the replacement of HPC blades in the CFM56-3 engine.

2. Maintenance, Repair and Overhaul Facilities

In order to maintain engines safe and functional, airliners must submit them to shop visits during their life cycle. In these visits, the engines are subjected to actions that can be of three levels: (1) Preventive maintenance: where the equipment is maintained before break down occurs; (2) Operational maintenance: where equipment is maintained while being used; (3) Corrective maintenance: where the equipment is maintained after break down occurs.

TAP M&E, an MRO facility based in Lisbon, Portugal, performs mostly preventive and corrective maintenance to the engines. The 2014's quality report [2] reveals that the CFM56-3 engine was the third more represented in the engine shop that year, as represented in Figure 1.

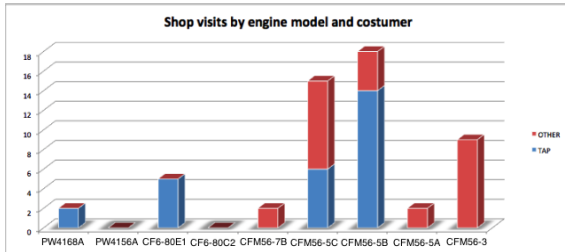


Figure 1: TAP M&E engine shop visits in 2014 [2].

2.1. TAP Test Bed

The design and conception of an aircraft engine is a long process, during which multiple intermediate designs are created. Having a test bed is then critical to test preliminary designs to improve the final design of an engine. The utility of a test bed does not end there, it is still needed after an engine entry in service. In MRO facilities, an acceptance test is conducted to reveal the condition and performance level of an engine after a maintenance intervention. That same test will define the workscope in an engine maintenance, repair and overhaul operation. TAP M&E's test cell is an 'L' type cell and its schematic is presented in Figure 2. It has a cross section of approximately 8.65m X 9.75m. The facility uses down-draft inlet with turning vanes as it can be seen in the left side of Figure 2. The incoming flow passes through noise reduction splitters and a bird screen before entering the working section of the test cell. Once the flow passed the working section, the exhaust gases pass rearward through a conventional cylindrical augmenter with a wedge diffuser section and then upwards through a folded vertical exhaust stack [1].

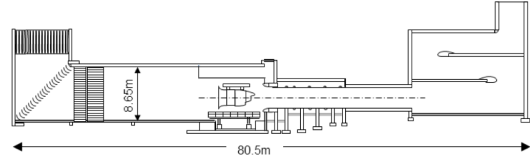


Figure 2: TAP test cell [1].

2.2. Test Bed Limitations

The purpose of a test cell is to acquire data from the tested engines. In order to make a good performance analysis, it is required to know which measurements are made in order to understand which are the limitations of the test cell. A description of this point will be made based on the work of [3] and [4].

The difficulty of calculating or measuring some parameters, e.g. the primary or core mass flow, introduces limitations such as: (1) Difficulties obtaining the combustion chamber exit temperature, T_4 , owing to the strong temperature gradients and high pressures felt in that area; (2) Study the separate relationship between the LPT and HPT with the overall engine performance is not possible since the only sensor located in that area is used to measure the Exhaust Gas Temperature (EGT), that is measured in the vane of the second stage of the LPT; (3) Obtain the bleed flow between the Booster (IPC) and the High pressure compressor, HPC, accurately is not possible, to calculate this parameter, deeper knowledge about the air system would be required; (4) The difficulty in placing sensors in the secondary flow duct, due to high pressure drag the sensors can separate from engine and go downstream, leads to lack of knowledge about the parameters of this area; (5) The difficulty in placing sensors between the booster's exit and the HPC's entry, this station is essential to isolate the Booster from the HPC in order to study their relationships with the engine performance [3].

2.3. Measured Parameters in TAP Test Bed

A test cell has the primary objective of measuring and recording data about the engine operation, usually, an engine is tested in a sequence of five operating points. Firstly, the engine is tested for two low rotation operating points, to check the engine condition. The rotational speed is then raised to speeds near the maximum for which the engine is certified to test the performance of the engine in three high-thrust regimes: maximum continuous (M/C#1), take-off (T/O) and back to maximum continuous (M/C#2). The measured parameters in TAP test bed are presented in Table 1.

Note that all the temperatures are total temperatures, as indicated by the prefix TT, and that PS and PT are static and total pressures, respectively.

Variable	Unit	Position
TT2	°C	Inlet fan
PT2	psia	Inlet fan
EGTK3	K	LPT 2nd stage vane
PS3	psia	Inlet combustion chamber
PT495	psia	LPT 2nd stage vane
PT25	psia	Outlet Booster
TT25	K	Outlet Booster
TT54	K	Outlet LPT
PT54	psia	Outlet LPT

Table 1: Measured parameters in TAP test bed

The EGT value is also referent to a total temperature. Apart from pressures and temperatures, the test cell also measures relative humidity (HR), total engine air mass flow (W2), specific fuel consumption (SFC) and high and low pressure spool speeds, N1 and N2, respectively.

3. Principles of Aircraft Engines

Gas turbine engines exist in many configurations, depending on their role. Different configurations are needed since there is a wide range of operating roles of aircrafts. The CFM56-3 engine is a turbofan engine. These engines are derived from the turbojet engine, with the intention of reducing the mean exit air velocity [5]. The main difference is that a turbofan engine has two gas paths instead of a single one as in the turbojet engines. While the primary flow, which flows through the core of the engine, is maintained, the secondary flow is accelerated by the fan and flows through the by-pass duct.

3.1. Deterioration of Aircraft Engine Components

It is a known fact that gas turbines, during normal operation, suffer deterioration like any other mechanical device. Gas turbine are particularly subjected to deterioration as they operate over a wide range of temperatures, pressures, speeds, loads and environments. All these deviations from design point cause a deterioration of the gas turbine performance, which can be defined as the cumulative effect of the performance degradations of various modules that constitute the engine, which are themselves composed of components such as blades, casings and spools.

The four major causes of engine degradation are: (1) Flight loads which are responsible for rubbing contact on any of the seals between the static and rotating parts of the engine; (2) Thermal distortion caused by changes in the original temperature pattern of the turbine inlet; (3) Erosion of aerofoils in compressor or turbine blades and outer seals; (4) Deposits, several particles enter the engine along with the air and are deposited on the different com-

ponents, these particles can also deposit in the cooling air ports, reducing the cooling air flow. Turbofan engines produce the thrust by accelerating a mass of air, they are air breathing machines. The air ingested by the engine is not clear of solid particles, such as dust. The ingestion of solid particles will affect the engine long term performance. The mechanism of dust ingestion by a turbofan engine is represented in Figure 3.

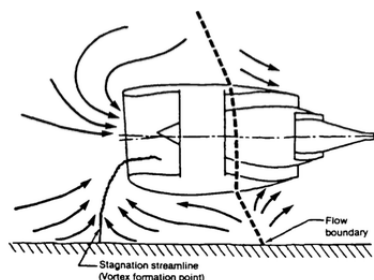


Figure 3: Dust ingestion in a turbine due to ground vortex formation [6].

Having different inertia, air and solid particles, such as dust particles, experience different accelerations and turning angles, which prevents them from following the flow of air through the blade passages, making them impact the blades surface and the inner and the outer annulus, increasing their pitting and roughness. This alters the pressure distribution on the blades surface, therefore reducing its performance. Blade chord restoration and refurbishment of blade surface are required after some operation time and can be conducted in MRO facilities such as TAP M&E [?].

The last effect of the impact of particles on compressor blades is the increase in clearance between the compressor blade rows and casings. Tip clearance increase of HPC blades is a consequence of three mechanisms: (1) The trench dug in the rub strip during engine transient manoeuvres; (2) Erosion of rub strip; (3) Loss of blade length. The tip clearance increase mechanism is illustrated in Figure 4.

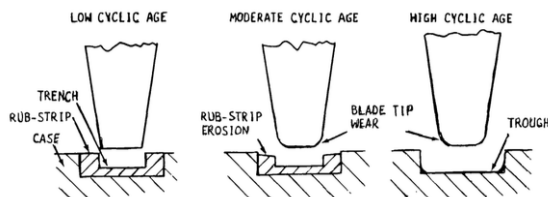


Figure 4: Evolution of erosion on HPC blades and rub-strips [6].

4. Modelling of the CFM56-3 Engine

4.1. The CFM56-3 Engine

The CFM56-3 engine was developed to incorporate in the Boeing 737. It is a high by-pass ratio (5:1), has two spools and axial flow. The engine has a very simple and robust design when compared with its antecessor, the CF6. Its small length gives it robustness, making it possible to reduce to two the number of frames supporting the engine. A cut-out of the engine is presented in Figure 5.

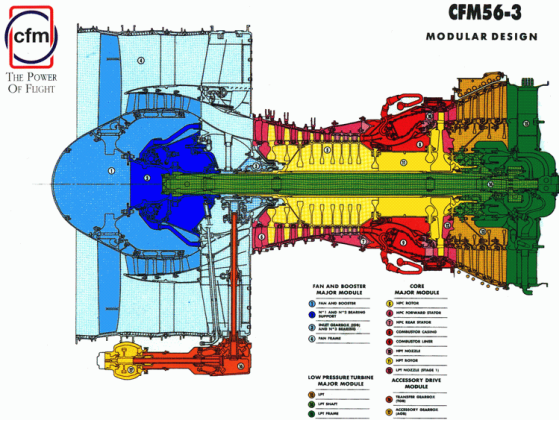


Figure 5: CFM56-3 schematic [8].

4.2. Thermodynamic Stations

As stated in Section 3, a turbofan engine has two gas paths. In order to estimate the performance of an engine, measurements in specific places across these two gas paths must be made. Such places are called thermodynamic stations and are represented in Figure 6.

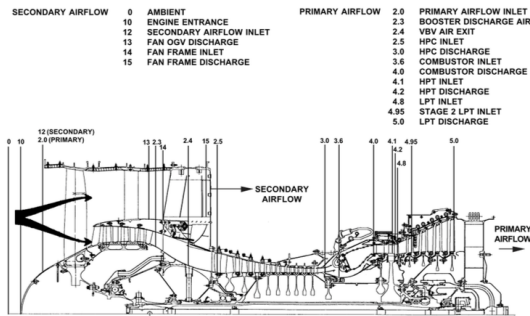


Figure 6: CFM56-3 thermodynamic stations [3].

4.3. Correlation Test Report

The most important information for modelling an engine is to have reliable test data, without this information is not possible to model the engine since the modelling process consists in adapting a standard engine model to simulate the tested engine data.

The source of the data used in this thesis is a document composed by CFMI in 1991 named Cor-

relation Test Report (CTR) [1]. The purpose of this document was to perform the correlation of the TAP M&E test cell, in which the performance of the correlation engine tested in TAP M&E test bed is compared with its performance in CFM test bed. The engine used produced reliable data for being a stable engine, an engine whose parameters were known and had small variations. The engine used in for the correlation is highly instrumented when compared with an engine coming to TAP M&E facilities. The raw test data presented in the report was gathered across 41 operating points as presented in reference [4].

The CTR does not present corrected temperatures and pressures, they must be corrected for Standard Day (SD) conditions first using Equations (1) and (2).

$$T_{corrected} = \frac{T2_{read}}{\Theta}, \quad (1)$$

$$P_{corrected} = \frac{P2_{read}}{\delta}, \quad (2)$$

where the temperature and pressure ratios are defined, respectively, as $\Theta = T2_{read}/T_{ambStd}$ and $\delta = P2_{read}/P_{ambStd}$. The *ambStd* subscript refer to the International Standard Atmosphere (ISA) values of temperature and pressure, which are 288.15K and 101.325kPa, respectively.

4.4. Method for Modelling an Aero Engine in Gas-Turb

GasTurb is a gas turbine performance calculation software developed by Kurzke [9]. With it, users can evaluate easily the thermodynamic cycle of the most common gas turbine architectures, both for engine design and off-design conditions. From the architectures available in the software, the one that is more suited for modelling the CFM56-3 engine is the *Geared Unmixed Flow Turbofan*, since it is the one which has a Booster.

The model is developed by matching the performance of a standard two spool turbofan engine presented by the software to the performance of the engines whose test data is available [10]. For this thesis the correlation test report [1] is the main source of test data.

Design Point The cycle reference point (CRP) is a single point chosen from the 41 operating points presented in the correlation test report. Choosing the point requires some care. The CFM56-3 engine has variable geometry from low to medium thrust-ratings. The uncertainty about the exact positioning of the moving parts, such as the variable bleed valves (VBVs) and variable stator vanes (VSVs), directs the choice of the design point to a high thrust-rating point.

The calculation of the CRP is made by iterating the unknown parameters providing GasTurb with known parameters taken from [1]. The results of the iterations are presented in Figure 7.

```

Iteration converged after 1 loops.

Iteration Variables:
1: Isentr.IPC Efficiency (0,85...0,95) = 0,877601
2: Isentr.HPC Efficiency (0,85...0,95) = 0,867732
3: Burner Exit Temperature K (1550...1700) = 1577,62
4: Isentr.LPT Efficiency (0,85...0,95) = 0,871299
5: Design Bypass Ratio (4,8...5,5) = 4,93858
6: Bypass Duct Pressure Ratio (0...2) = 0,982605
7: Design Core Nozzle Angle [°] (0...10) = 6,05991

Iteration Targets:
1: Booster Exit Temp T24 = 369,92
2: HPC Exit Temperature T3 = 770,8
3: Fuel Flow = 1,0951
4: LPT Exit Pressure P5 = 148,131
5: LPT Exit Temperature T5 = 862,6
6: Bypass Nozzle Area = 0,74236
7: Core Nozzle Area = 0,2933

```

Figure 7: Iterations results.

The calculations converged after a single loop, respecting all the targets and all the iterated values are within reasonable ranges for each of them.

Off-design Modelling The Off-design performance modelling is where the software standard component maps are adapted to the correlation test data. These maps represent the relationships between corrected flow, corrected speed, pressure ratio, and temperature ratio (or efficiency) of a turbo-machine. A Booster compressor map is represented in Figure 8.

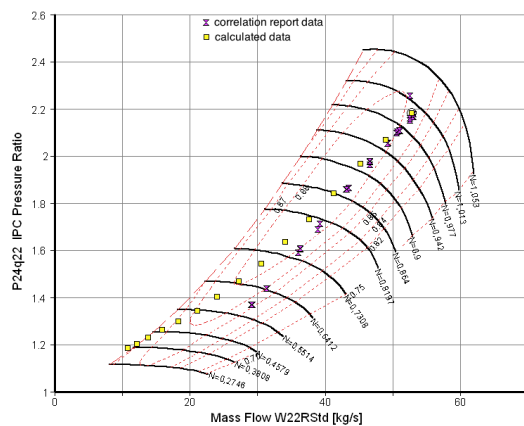


Figure 8: Booster map with operating line printed.

Since the engine manufacturers do not reveal to the general public informations about the engines performance, the solution is to use the generic component maps provided by GasTurb and to adapt them to the Correlation Test Report data, following the procedure described in references [11, 10]. The procedure presented in [11, 10] was improved by Kurzke in [12] with the addition of hybrid data, which is simply additional data that, even though it is not present in [1], can be calculated from data

present in the same document. The purple points represented in Figure 8 are an example of hybrid data. Printing them was only possible by estimating the Booster pressure ratio (P_{24}/P_{22}) and corrected mass flow (W_{22RStd}) from the available data present in [1].

4.5. Verification and Validation

According to reference [12], there are three important criteria to validate the model: (1) the SFC versus Engine Corrected Air Flow curve; (2) the accuracy of the exhaust gas temperature; (3) the accuracy of the LPT exit temperature, T_5 .

The SFC curve calculated by GasTurb agrees well with the measured data for corrected engine flows above 240kg/s (thrust values above 57kN). Below that value, the results are not precise due to the action of the HPT clearance control system, which causes the step in the SFC curve, as represented in Figure 9.

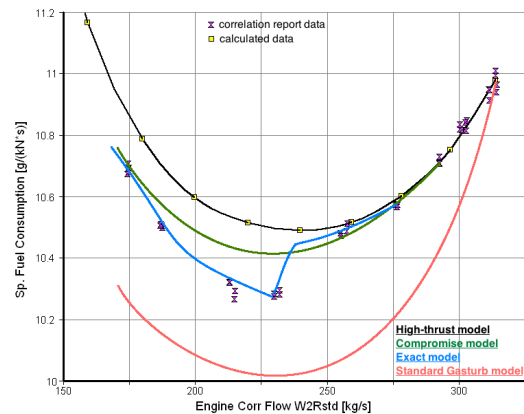


Figure 9: SFC curve for different types of models.

Performance models can be of three types: (1) Compromise model, if the model tries to be precise at low and high spool rotations; (2) Exact model, precise for all the operation range; (3) High-thrust model, precise for high-thrust ratings. Figure 9 reveals that the developed model (black line) is a high-thrust model. This result is acceptable since the performance of an engine is critical for thrust-ratings above 80% of the T/O thrust. Thus, the model is suited for performance studies.

Once the agreement of the SFC curve is confirmed, the next thing to do is to check the model simulation of the EGT, as shown in Figure 10.

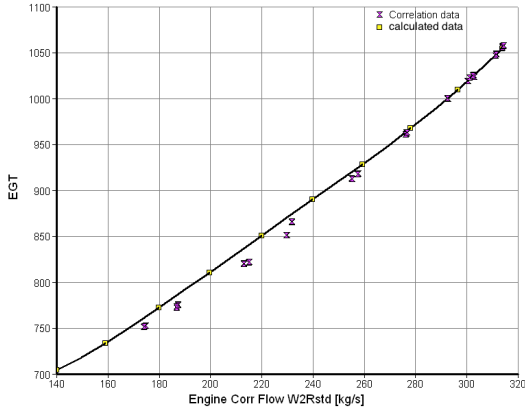


Figure 10: Comparison between measured and calculated EGT.

Figure 10 shows exactly what was expected: high accuracy for values of corrected engine flow above 230kg/s and a deviation below that point, of about 10K. For being both related to the LPT, T5 and EGT are related and their simulations have similar accuracies. For that reason, the T5 simulation results will not be presented.

5. Application of the Model

The performance model developed may now be used to study the performance of CFM56-3 engines coming to TAP M&E facilities, estimating the degradations of the engines tested. The model will be used to estimate the HPC performance increase of an engine that had the blades from the first three stages of its HPC exchanged for new ones. To do so, a GasTurb tool called Model Based Test Analysis (MBTA) will be necessary. This tool allows the user to introduce a set of data measured in test bed to estimate the deviations in components performance between the tested engine and the performance model, the benchmark.

Data from the three high thrust-rating operating points introduced in Subsection 2.3 will be used. Comparison between the data required by GasTurb and the data measured in TAP M&E test cell reveals that some of the required parameters are not among the measured ones or are incoherent. These parameters are: T17, P17, T25, P25, P45, T45, P5 and T5, located in the outlets of the Fan, Booster, HPT and LPT, respectively.

Model Based Test Analysis tool offers the user the option to perform iteration to find missing values, however, this action has a toll on the simulation. To do so, the user has to fix a component performance relatively to the performance of that same component in the correlation engine.

5.1. Engine Performances Comparison

Once the needed model data is introduced in the MBTA input window and the iterations are defined,

the results in Figure 11, for engine A (before chord length restoration) are obtained:

Fan Flow Factor	0,996659	
Fan Outer Efficiency Factor	1	
Fan Inner Efficiency Factor	1,01472	
Booster Flow Factor	1	
Booster Efficiency Factor	1	
HPC Flow Factor	1,06667	
HPC Efficiency Factor	0,976717	
HP Turbine Flow Factor	1,05496	
HP Turbine Efficiency Factor	1,03501	
LP Turbine Flow Factor	1,01216	
LP Turbine Efficiency Factor	0,97775	
Core Nozzle Area Factor	1,01698	
Bypass Nozzle Area Factor	0,978485	
Gross Thrust Factor	0,964041	
T45 measured - T45 calculated	K	0,00841076
T5 measured - T5 calculated	K	-8,85389

Figure 11: MBTA results for engine A at M/C#1.

Additionally, the deviation in EGT can be studied to measure the accuracy of the method used. The calculated value in MBTA was 1085.82 K and the measured value in Test bed was 1086.61 K, the corresponding relative error is 0.073%. From Figure 11, it is possible to see that the engine tested did not perform as the benchmark engine did, otherwise the efficiency and flow factors would be equal to one. To make a complete study of the HPC, independent from the model, information about station 25 would be needed, as stated by Ridaura [4]. Both the T25 and P25 sensor had invalid measurements in both tests. Repeating the procedure to the two other operating points (M/C#2 and T/O#1) for engine A and equally for the same three operating points for engine B (after the blades substitution) leads to results presented in Figure 12 and in Table 3. From

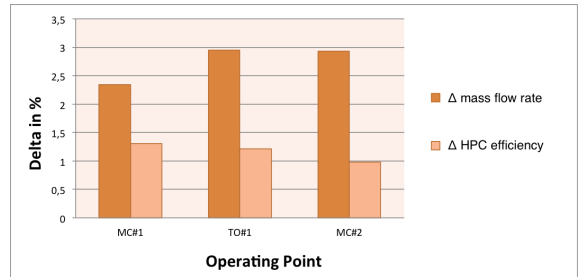


Figure 12: Variation of HPC efficiency and capacity.

Figure 12, it is possible to conclude that the raise in efficiency and capacity in the HPC was similar for the different operating points that were simulated in the MBTA. The increase in these factors from engine A to B was expected since engine A had damaged blades (reduced chord length) which later were replaced by new ones. Further analysis of Table 3 reveals that, in terms of EGT, the results are close for the two Maximum continuous points simulated in the MBTA but the results for the Take Off point are farther from the measured value in TAP M&E test cell. The Take-off (T/O # 1) point is immediately excluded for having the largest discrepancies in the EGT values. The reason

Engine A		
Operating Point	EGT_{mea} (K)	EGT_{calc} (K)
M/C#1	1084.94	1086.32
T/O#1	1113.72	1080.12
M/C#2	1086.61	1084.64

Engine B		
Operating Point	EGT_{mea} (K)	EGT_{calc} (K)
M/C#1	1076.67	1068.28
T/O#1	1103.17	1083.35
M/C#2	1071.00	1080.59

Table 2: Results of the test runs simulations.

for this deviation may be related to the modelling of the engine. The correlation engine was tested for N1R values from 3000rpm to 4835rpm, the latter value corresponding to 100% of the engine loading. However, when TAP M&E tests an engine at T/O rating, it is usual to raise N1R to 105%, which falls out of the domain where the engine performance was modelled. Both the Maximum continuous points produced good EGT estimations but the best results belong to the first point, M/C # 1.

In order to develop the tool to study the HPC blade replacement, the performance improvement from Engine A to B must be estimated. Thus, one of the three operating points must be chosen as the reference. With the take-off operating point already excluded, the choice is between the two M/C points. Such choice will be made in Subsection 5.3

5.2. Engine Sensitivity to Components Performance

Sensitivity studies is the GasTurb tool to study the effects of small changes of some of the engine parameters on the others. It can be very useful to study how important one or the other input quantity is for a certain cycle, e.g. it is possible to compare the effect of degradations of two different components on EGT: a 1% efficiency degradation in HPC or the same degradation in the HPT. It is possible to study which component's degradation affects EGT the most. A sensitivity study can solve that and many other problems [9]. Tables 3 and 4 represent the results of a sensitivity test, where the effects of 1% variations in the efficiencies of the LPC, Booster, HPC, HPT and LPT on T45, T5, Net Thrust and SFC. Additionally, using the results for T45 and T5 will allow to study the effect of the 1% variations in the components efficiency in the EGT, making use of Equation (3).

$$EGT = 0.976 * [T45 - 0.217 * (T45 - T5)]. \quad (3)$$

The results from the sensitivity study conducted in the correlation engine model, represented in Ta-

Degradation	$\Delta NetThrust_{1\%}$ (KN)	$\Delta SFC_{1\%}$ (g/(h KN))
$\Delta\eta_{LPC}$	-0.22	-0.73
$\Delta\eta_{IPC}$	-0.06	-0.28
$\Delta\eta_{HPC}$	-0.02	-0.69
$\Delta\eta_{HPT}$	-0.02	-0.84
$\Delta\eta_{LPT}$	-0.33	-1.04

Table 3: Sensitivity of net thrust and SFC to component degradation.

Degradation	$\Delta T45_{1\%}$ (K)	$\Delta T5_{1\%}$ (K)	$\Delta EGT_{1\%}$ (K)
$\Delta\eta_{LPC}$	-4.09	-3.02	-3.762
$\Delta\eta_{IPC}$	-3.23	-2.57	-3.010
$\Delta\eta_{HPC}$	-8.17	-6.81	-7.683
$\Delta\eta_{HPT}$	-12.61	-10.58	-11.874
$\Delta\eta_{LPT}$	-5.88	-7.85	-6.153

Table 4: Sensitivity of T45, T5 and EGT to component degradation.

bles 3 and 4, provide some important conclusions about the engine behaviour:

- Changing a component efficiency will bring modifications to the whole engine. T45 and T5 are measured respectively before and after the HPT and yet they are influenced by changes in the Fan efficiency;
- The high pressure components, HPC and HPT, are the one that influence T45 and T5 the most. Thus, they will also influence EGT the most;
- A 1% efficiency loss in the HPT leads to an incredible loss in EGT margin of almost 12 degrees Celsius;
- Net thrust remains practically unchanged when an efficiency is changed. This parameter is influenced by changes in flow, specially in the Fan (1% increase in Fan capacity lead to an increase of 2.06kN);
- Changing the components efficiency brings changes to the Fuel Flow, observable by the changes in SFC, which is directly connected to Fuel Flow and Net thrust (which remained almost unchanged).

5.3. Replication of MBTA Results using Engine Sensitivities

The combination of the results from Figure 12 and Table 4 can be used to estimate the EGT from engine A to B, for the two M/C points in study. The EGT drop will be estimated using Equations (4a) and (4b):

$$T_{final} = \Delta T + T_{initial}, \quad (4a)$$

$$\Delta T = \Delta\eta * \Delta T_{1\%}, \quad (4b)$$

where $\Delta\eta$ is the difference between the HPC efficiency factor from engine A to B, 1.31%. Equations (4) are used twice, one time for T45 and the other for T5. The resultant temperatures are then introduced in Equation (3) which will provide the the EGT values before and after the repair. The results of this study are presented in Table 5.

Operating Point	$\Delta EGT_{calc}(K)$	$\Delta EGT_{mea}(K)$
M/C#1	-9.737	-9.944
M/C#2	-7.732	-13.944

Table 5: EGT variation from engine A to B.

Table 5 reveals a great discrepancy between the results for the two operating points used. This discrepancy may be explained by the difference between the calculated $\Delta\eta_{HPC}$ between the two operating points (1.31% M/C#1 and 0.98% for M/C#2), as illustrated in Figure 12.

6. Performance Studies

6.1. Effects of Stage Efficiency Modifications on Overall Compressor Efficiency

The results from the past chapters will now be used to develop a tool to help TAP M&E improve its maintenance and overhaul actions on the HPC of CFM56-3 engines. In order to understand how to maintain the HPC in an efficient way, knowing the relation between stage and overall efficiencies is mandatory. Since the HPC stages are different from each other, it is expected that different stages have different influences on the overall compressor efficiency.

The influence of stage efficiency on the overall efficiency will be conducted studying only the first three stages of the CFM56-3 HPC. This simplification is acceptable since only the first three stages of the HPC were modified, while all the others remained unchanged.

From the diagram of forces acting on the cascade, presented in Figure 13, the static pressure rise across the stage is defined as

$$\Delta p = 0,5\rho V_a^2(\tan^2 \alpha_1 - \tan^2 \alpha_2) - \bar{\omega}. \quad (5)$$

where $\bar{\omega}$ are the static pressure loss coefficient and V_a is the axial velocity, which is assumed constant and α_1 and α_2 are the angles between the axial direction and a tangent to the leading and trailing edges of the blades, respectively.

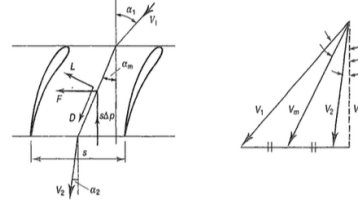


Figure 13: Forces acting on a cascade [5].

The force per unit length acting along the cascade is defined as $F = S\rho V_a^2(\tan \alpha_1 - \tan \alpha_2)$, where S is the spacing between consecutive blades.

Drag and lift forces are defined along and perpendicular to the direction defined by the mean velocity, defined as $V_m = V_a \sec \alpha_m$, where the mean angle (α_m) is given by $\tan \alpha_m = 0.5(\tan \alpha_1 + \tan \alpha_2)$. Resolving along that direction gives

$$D = 0.5\rho c V_m^2 C_{DP} = F \sin \alpha_m - S\Delta p \cos \alpha_m, \quad (6)$$

Combining Equation (6) with Equation (5) and the force per unit length leads to

$$C_{DP} = \left(\frac{S}{c}\right) \left(\frac{\bar{\omega}}{0.5\rho V_1^2}\right) \left(\frac{\cos^3 \alpha_m}{\cos^2 \alpha_1}\right). \quad (7)$$

Repeating for the perpendicular direction results in

$$L = 0.5\rho c V_m^2 C_L = F \cos \alpha_m + S\Delta p \sin \alpha_m, \quad (8a)$$

$$C_L = 2 \left(\frac{S}{c}\right) (\tan \alpha_1 - \tan \alpha_2) \cos \alpha_m - C_{DP} \tan \alpha_m. \quad (8b)$$

Vavra [13] states that the overall drag coefficient (C_D) is defined as the sum of three contributions: (1) Profile drag coefficient (C_{DP}), whose value is read from Figure 14; (2) Annulus drag coefficient, defined as $C_{DA} = 0.020(S/h)$; (3) Secondary drag coefficient, given by Equation (9).

$$C_{DS} = \left(0.25 \frac{\delta}{S \cos \alpha_2} + 0.055\right) C_L^2 \left(\frac{c}{h}\right). \quad (9)$$

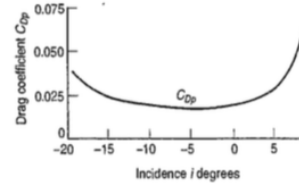


Figure 14: Profile drag coefficient versus incidence angle i [5].

The value for the profile drag coefficient defined before for a two-dimensional cascade, apply equally for the annular case if C_D is substituted for C_{DP} .

Thus, for the annular cascade, C_D is given by Equation (7).

The stage pressure ratio (R_S) for each stage will be introduced in $\eta_{is,c} = \frac{T_{01}}{T_{02}-T_{01}} \left[\left(\frac{p_{02}}{p_{01}} \right)^{\frac{\gamma-1}{\gamma}} - 1 \right]$ to calculate the overall compressor efficiency. The stage pressure ratio is calculated using Equation (10).

$$R_S = \left[1 + \frac{\eta_S \Delta T_{0S}}{T_1} \right]^{\gamma/(\gamma-1)}, \quad (10)$$

where ΔT_{0S} is stage temperature rise and η_S is the stage efficiency of the blade row, defined as

$$\eta_S = \frac{\Delta p_{th} - \bar{\omega}}{\Delta p_{th}} = 1 - \frac{\bar{\omega}/0.5\rho V_1^2}{\Delta p_{th}/0.5\rho V_1^2}, \quad (11)$$

where Δp_{th} is the theoretical pressure rise in the blade row. In terms of the inlet dynamic head and cascade air inlet and outlet angles, is given by

$$\Delta p_{th} = 0.5\rho V_1^2 \left(1 - \frac{\cos^2 \alpha_1}{\cos^2 \alpha_2} \right). \quad (12)$$

6.2. Geometrical Blade Rows Measurements

The calculation of the stage efficiencies require some geometric data from the blade rows. The measured parameters were the blade height (h), the blade spacing (S), the leading edge angle and the trailing edge angle. The measurements made on the first three rotor stages are presented in Table 6.

Stage	α_1 (degrees)	α_2 (degrees)	h (in)	S (in)
1	66.185	51.626	3.360	1.439
2	72.407	44.900	2.574	1.032
2	71.289	45.014	2.000	0.908

Table 6: Measurements performed on the HPC.

6.3. Results

The methodology described in Section 6.1 is then applied for engine in study, the CFM56-3 engine.

It is possible to study the influence of the different stages on the overall efficiency of the HPC. Changing by steps of -0.01 the efficiency of each stage, one at a time, leads to the results presented in Figure 15.

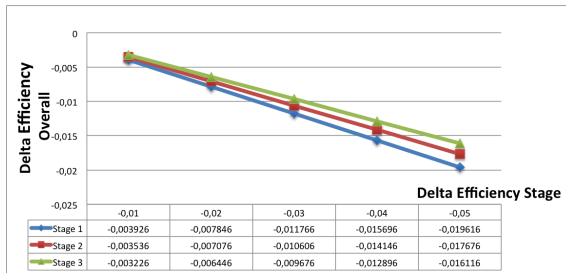


Figure 15: Stage efficiency influence on overall efficiency.

6.4. Effects of Tip Clearance Modifications on Overall Compressor Efficiency

The increase in tip clearance is a common deterioration in both compressor and turbines [6], the clearance between the wing tip and the annulus wall allows the air to escape between them just like in an aircraft blade tip, creating tip vortices. Tip clearance influences the overall efficiency of the compressor by increasing the end losses which, consequently, increases the loss factor of the different stages.

Results In order to study which stage influences the overall performance the most, the effects of 1% tip clearance reduction in each stage were studied. The results are presented in Table 7.

Stage	δ_{Stg}/h_{Stg}	δ_{Stg}	C_{DS}	$\Delta\eta_{OVR}$	Cost (\$)	$\Delta\eta_{OVR}/Cost$
1	0.01	0.034	0.012	0.425	43325	0.010
2	0.01	0.026	0.060	0.760	30905	0.025
3	0.01	0.020	0.061	0.669	27040	0.025

Table 7: Results of the simulation of the tip clearance reduction.

From Table 7 it is possible to conclude that the second and third stages influence the overall efficiency the most, for a given tip clearance.

The tool that will now be developed will map the performance degradation of the HPC for several combinations of tip clearances in the first three stages. It will be assumed that the shape of the blade remains constant, i.e., only the height of the blade will be reduced. According to Vavra [13], usual tip clearance in a compressor stage range from 1% to 2% of the average blade height of that same stage. It will be assumed that the engine with the old blades has tip clearance equal to 2% of the blades height in each stage and that with new blades has that value reduced to 0.5%. With the introduction of two additional intermediate points the total of combinations possible is 64.

An excerpt of the complete map is presented in Figure 16.

% blades exchanged	Delta eff %	Cost	Delta eff/cost
100-100-100	2,7844	153 213	0,0182
100-100-67	2,4492	139 693	0,0175
100-100-33	2,1138	126 173	0,0168
100-100-0	1,7781	112 653	0,0158
100-67-100	2,4034	137 319	0,0175

Figure 16: Excerpt of the complete map of performance increase vs repair costs.

7. Conclusions

Gas turbine manufacturers only publish some information and test data for the commercial gas turbines, which only give little information about that specific machine. The main objective for this thesis

was to provide TAP M&E additional information about the internal relations on a specific engine, the widely used CFM56-3 engine. The modelling software chosen was GasTurb, which provides the user the possibility to model his own engine, using his own data.

In order to model an engine, model data has to be fitted to match the available test bed data. The modelling procedure is divided in two main parts: design point calculations and off-design performance matching. The use of a different point from the one used by Ridaura [4] lead to a better estimation of the engine by-pass ratio, which consequently lead to better estimations of the core and by-pass flows and components efficiencies. The off-design model of the engine was developed and optimized for high-thrust ratings, where the performance of the engine is critical. The developed model is able to simulate the correlation engine with great precision for thrust ratings over 80% of the design point rating.

The model was then tested studying the performance improvement in an engine which had the blades from the first three stages of its HPC exchanged for new ones. The results were that the engine its HPC efficiency improved by 1.31%. The precision of the model was tested by comparing the calculated values of the EGT with the measured values during the two test runs, resulting in deviations in the order of 1%. However, these analyses are still limited due to some of the data not being measured in the test bed. The data must then be taken from the model and adapted to each engine.

The sensitivity studies were then used to validate the results from the MBTA. The EGT of the engine A (before the blades replacement) was improved using the results from the Sensitivity tests and the resulting EGT drop from engine A to B calculated using engine sensitivities deviated only 2.08% from the measured EGT drop in the test cell.

The effects of two common HPC blades degradations were then studied: the reduction in chord length and the increase in tip clearance.

Studying the influence of blade chord length reduction on overall compressor efficiency was not possible due to the impossibility of estimating the C_{DP} of an eroded HPC blade.

The effect of tip clearance in the different stages of the HPC was studied for 64 combination of tip clearances between 0.5% and 2% of the blades height. This study resulted in the conclusion that, due to the higher deflection imposed to the air in these stages, the second and third stages influence the overall compressor efficiency the most, for a given tip clearance value.

This thesis provided TAP M&E with some very useful tools that will help estimating the perfor-

mance of the engines coming to the shop and, consequently, save both financial and human resources.

References

- [1] P. Compenat, F. Trimouille, and approved by R. Mougnot. Correlation Report of TAP Air Portugal for CFM56-3 engine. Technical report, CFM, 1991.
- [2] TAP quality report, company confidential. Technical report, TAP, 2015.
- [3] Antnio Miguel Abreu Ribeiro Henriques. Anlise da influencia dos procedimentos de manuteno do motor CFM56-3 no seu desempenho no banco de ensaios. TAP Portugal, 2011.
- [4] J. A. R. Ridaura. Correlation analysis between hpc blade chord and compressor efficiency for the cfm56-3. Master's thesis, Instituto Superior Tcnico, October 2014.
- [5] H. Cohen, G.F.C. Rogers, and H.I.H. Saravanamuttoo. *Gas Turbine Theory*. Longman Group Limited, fourth edition, 1996. ISBN 0 582 23632 0.
- [6] M. S. Grewal. *GAS TURBINE ENGINE PERFORMANCE DETERIORATION MODELLING AND ANALYSIS*. PhD thesis, Cranfield Institute of Technology, School of Mechanical Engineering, February 1988.
- [7] F. M. White. *Fluid Mechanics*. McGraw Hill, 7th edition, 2011. ISBN 978-0-07-352934-9.
- [8] CFM. *CFM56-3 Basic Engine, B737-300. Formao Profissional TAP. Revision 3*. 1992.
- [9] Joachim Kurzke. *Gasturb 11: Design and Off-Design Performance of Gas Turbines*. 2011.
- [10] Hannes Wemming. Validation and integration of a rubber engine model into an MDO environment. Master's thesis, Linkoping University, 2010.
- [11] Joachim Kurzke. How to create a performance model of a gas turbine from a limited amount of information. ASME Turbo Expo 2005: Power for Land, Sea and Air. *American Society of Mechanical Engineers*, 2005.
- [12] Joachim Kurzke. CFM56-3 in TAP. Confidential document.
- [13] M. H. Vavra. *Aero-thermodynamics and Flow in Turbomachines*. John Wiley & Sons, 1st edition, 1960. ISBN 10: 0882751891 / ISBN 13: 9780882751894.